ELSEVIER

Journal of Power Sources 56 (1995) 179–187

JOURNAL OF POWER SOURCES

A metal-free polypyrrole/graphite secondary battery with an anion shuttle mechanism

Tammo Boinowitz, Gerd tom Suden, Ulf Tormin, Holger Krohn, Fritz Beck *

Universität Duisburg, Fachgebiet Elektrochemie, Lotharstrasse 1, 47057 Duisburg, Germany

Received 5 April 1995; revised 21 August 1995; accepted 23 August 1995

Abstract

A novel secondary battery with a porous, doped polypyrrole layer (PPy) (nominal thickness 100–300 μm) as the negative electrode and a pristine composite 80 wt.% natural graphite/20 wt.% polypropylene (CPP) as the positive electrode is described in detail. The current collectors are fabricated of 24 wt.% carbon black/76 wt.% polypropylene. Thus, an entirely metal-free battery is fabricated. The optimum electrolyte is 0.2 M $LiClO_4$ in propylene carbonate, containing 20 mM water. The theoretical energy density is about 80 Wh kg^{-1} at a thermodynamic cell voltage of 1.7 V. Practical values of 20–30 Wh kg^{-1} are feasible for bipolar systems. 6 cm^2 and 20 cm^2 cells are galvanostatically cycled at 0.5 mA cm^{-2}. The cells are readily rechargeable, and an anion shuttle mechanism is operative. The Ah efficiency is more than 90%. The very positive potentials, which are attained on the positive electrode during the charge process (at about 2 V versus standard hydrogen electrode) lead to some losses due to the irreversible oxidation of the solvent molecules. Thus, redoping of PPy is not a quantitative process on discharge. As a consequence, negative capacity is lost in an early stage. Solvent/electrolyte systems with an improved anodic stability and eventually periodical full oxidation of the PPy may give a solution to this problem. The active mass utilization of the porous PPy layer is thoroughly optimized.

Keywords: Secondary batteries; Graphite; Polypyrrole

1. Introduction

Metals, predominantly commodity metals, are thermodynamic sources that are widely used in battery negatives since the early days of electrochemical energy storage [1]. As corrosion (self-discharge) is a general problem the use of metals such as iron, zinc and aluminium, is critical in rechargeable batteries. Lead and cadmium are preferred in aqueous electrolytes for their relative stability due to their high hydrogen overvoltage. However, environmental aspects and availability of these metals are severe limitations. Since about 20 years, lithium is regarded as an optimal source due to its very negative potential and low equivalent weight m_e. The necessity to use aprotic solvent/electrolyte systems as well as security problems hamper, up to now, the development of large accumulators based on lithium. The extreme reactivity of this metal forces one to use lithium compounds such as LiC_6 or LiAl [2,3], which provide only about 10% of the original m_e.

Entirely metal-free cells would solve these problems. They have been introduced as the quinone accumulator by several groups in the early 1970s [4–7]. The most practical system is derived from chloranil and anthraquinone. A decisive drawback, however, is a low voltage of about 0.5 V. We have analysed the potentialities of other metal-free systems [8–10]. One of them has (doped) polypyrrole as the negative and graphite (salts) as the positive electrodes. The overall reaction for perchlorate anions is as follows:

$$[C_{24}] + [-Py_3^+ - \cdot ClO_4^- \cdot \nu S]_{p/3} \underset{\text{discharge}}{\overset{\text{charge}}{\rightleftharpoons}} [C_{24}^+ ClO_4^- \cdot \nu' S] + [-Py_3-]_{p/3} + (\nu - \nu')S \quad (1)$$

where Py means a monomer unit C_4H_3N in polypyrrole and S is the solvent molecule with the stoichiometric factors ν and ν'. Polypyrrole is a well-known conducting polymer, which was already used in rechargeable lithium batteries as a positive electrode in conjunction with a Li [11] or C_6Li [12] negative electrodes. The positive electrode in the present rechargeable cell is graphite, as mentioned above. It is transformed into a graphite intercalation compound of the acceptor-type upon charge. Such electrodes were already used in the lead/graphite [13,14], the palladium/graphite [15] and the graphite concentration cells [16]. The very

* Corresponding author.

SSDI 0378-7753(95)02262-F

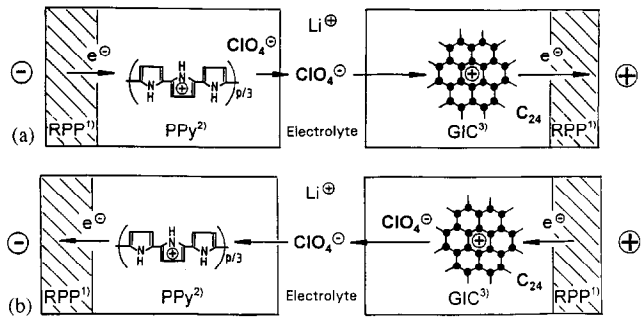

Fig. 1. Schematic representation of the (a) charge and (b) discharge processes in a PPy/GIC rechargeable cell.

positive potential of about 2.0 V versus standard hydrogen electrode (SHE) leads in the present combination to a theoretical cell voltage of 1.7 V. As both electrodes are positive to the hydrogen electrode, no hydrogen will be generated in the battery. Carbon black-filled polypropylene (RPP) is used as the current collector [8–10,17,18]. An entirely metal-free cell is, therefore, available.

The anion is either in the one or in the other host lattice, see Eq. (1). The anion shuttles are between the electrodes. This mechanism is schematically illustrated in Fig. 1. The cell is mounted with doped polypyrrole layers and pristine graphite.

Both forms are stable in the air. On charge, the anions leave the PPy host lattice and enter into the graphite. In the course of the discharge reaction, the anions go in the opposite way. Systems with a cation shuttle mechanism, predominantly Li^+ ions, are described in Refs. [2,3,19]. Albeit acid electrolytes as well as aprotic systems are possible, only the aprotic systems were studied.

After some preliminary publications in reviews [8–10] and conference proceedings [20,21], this paper describes the present development.

2. Experimental

The standard solvent/electrolyte system consisted of 0.2 M $LiClO_4$ (Riedel–de Haen, 99%) and propylene carbonate (PC) (Fluka, purum >99%), distilled at 94–95 °C, 15 mmHg. The water concentration was ~10–20 mM. The cycling experiments were performed at 20 °C under argon in a stagnant electrolyte. Current densities were mostly 0.5 mA cm^{-2}, and they were switched by an AMEL bigalvanostat Model 545, if necessary, in combination with a timer Indigel, IDE 546. Metal-free base electrodes RPP (current collectors) were fabricated from carbon black (24 wt.% Corax L (Degussa)) filled polypropylene (Novolen 1120 HX (BASF)). The positive active material was a composite electrode CPP, consisting of 80 wt.% natural graphite (Normalflocke (Kropfmühl)) and 20 wt.% polypropylene [22]. A 100 μm polypyrrole (PPy) layer was electrodeposited onto RPP at a current of 4 mA cm^{-2} from a bromide-containing electrolyte to yield the negative electrode [23]. The composition was 0.2 M $LiClO_4$/PC with 1 mM Br^- and 0.1 M pyrrole. The cells used for this purpose were similar to the cell with horizontal electrodes described in Refs. [24,25].

The cyclic behaviour of the single electrodes was investigated in the glass cells as previously done. A platinum sheet and a NaCl–saturated calomel electrode (+236 mV versus SHE) were used as the counter and reference electrodes, respectively.

Cycling experiments were performed in several types of cells, each equipped with vertical circular round electrodes of different surface areas. The 6 cm^2 version was fitted in a (horizontal) glass cylinder cell where they were sealed with the help of O-rings (perbunan) against the glass walls and the brass contacts. The distance between the electrodes was about 1 cm. A vertical tube was arranged in the middle of the electrolyte chamber to allow gas and liquid volumes to be measured. The 20 cm^2 model cell was constructed as a plate and frame design with polypropylene frames and perbunan gaskets. The electrolyte chambers were 1 mm thick and carried a 0.5 mm hole at their upper ends in order to change their volume and to fill them with a syringe. These elements were also used for a bipolar design. All measurements were performed at room temperature after thorough deaeration of the electrolyte by argon bubbling.

3. Results

The results are presented in four sections. Section 3.1 and 3.2 comprise the optimization of the single electrodes and their cyclic behaviour. Cells composed of these electrodes were cycled under a variety of conditions in monocells (Section 3.3) with an area of 6 and 20 cm^2. An array of 5 bipolar cells was assembled to a bipolar battery and cycled (Section 3.4).

Two figures-of-merit are used throughout, namely the current efficiency α on cycling and the active mass utilization μ. The former is defined according to:

$$\alpha = \frac{Q_{\text{disch}}}{Q_{\text{ch}}} \tag{2}$$

where Q_{ch} is the charge due to the charge reaction and Q_{disch} the charge for the discharge reaction in any cycling experiment. The active mass utilization μ is given by:

$$\mu = \frac{Q_{\text{disch}}}{Q_{\text{th}}} \tag{3}$$

where Q_{th} is the theoretical charge capacity for a 100% utilization of the active material according to Faraday's law.

3.1. Polypyrrole-negative electrode

A general strategy was followed-up for the fabrication of PPy porous layers on RPP. The PPy layer was directly deposited anodically on the current collector giving a better result

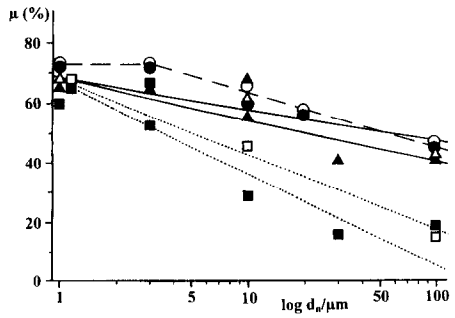

Fig. 2. Active mass utilization, μ, vs. logarithm of the nominal layer thickness, d_n, of porous PPy electrodes. Anodic deposition in PC with 0.1 M pyrrole and 0.2 M $LiClO_4$; $j = 4$ mA cm^{-2}. Cycling (0.5 mA cm^{-2}) in 0.2 M $LiClO_4$. The following substrate/solvent combinations were used. Bromide deposited (□) Pt/PC; (■) RPP/PC; (●) RPP/graphite felt. Not bromide deposited (△) Pt/acetonitrile; (▲) RPP/acetonitrile; (○) RPP/graphite felt in PC.

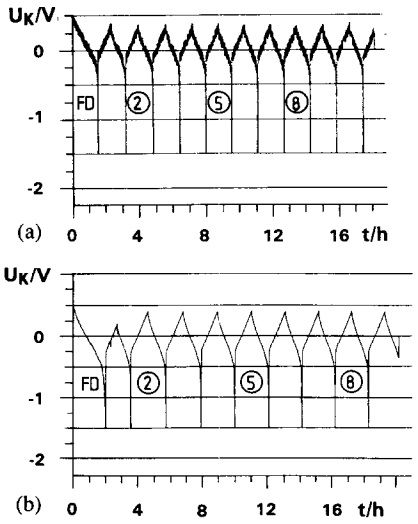

Fig. 3. Typical cyclic curves at $j = 0.5$ mA cm^{-2} for polypyrrole single electrodes in 0.2 M $LiClO_4$/PC. Potential limits: −1.5 V to +0.4 V vs. SCE: (a) electrodeposition under bromide catalysis on RPP, and (b) electrodeposition without bromide catalysis on RPP/graphite felt. (FD = final discharge.)

Table 1
Influence of the solvent/electrolyte system (0.2 M $LiClO_4$) on the active mass utilization, μ, of polypyrrole. Potentiodynamic cycling, $v_s = 0.5$ mV s^{-1}, $y = 0.33$. Anodically deposited PPy layers (37 μm) (1,2), PPy-pellets in column (3) (after Ref. [26])

0.2 M $LiClO_4$ in solvent	PPy layers		PPy pellets [Ref. 26]
	Up to 1.65 V	For an extended potential range	
Acetonitrile	35%	65%	88%
Propylene carbonate	20%	40%	77%
Nitromethane	7%	14%	
Sulfolane	3%		12%

than the chemical production of PPy powders that are pressed to form pellets, see Ref. [26]. The following procedures were developed:

(i) Deposition at high current densities using bromide catalysis [27,28]. It was already observed by Bittihn and coworkers [11,29] that porous layers are formed at higher current densities, which allow the current density in the course of the cycling of the electrode to be increased. Bromide catalysis is used to avoid overoxidation in the course of filmforming electropolymerization.

(ii) Co-deposition of carbon black; this was thoroughly elaborated [23] and described in Refs. [30,31].

(iii) Graphite felt (Sigri GFD 2), contacted by RPP, is optimized in the authors' laboratory and described in Refs. [32,33].

More details of this preparation method are given in Refs. [23,34].

The ultimate goal was to fabricate porous electrodes by simple procedures, without complicated processes [35].

Pulse plating (time constants 1 and 0.1 s) was tried but the porosity of the electrode decreased and active mass utilization was relatively low.

Fig. 2 shows the active mass utilization of the PPy-layers versus nominal thickness (d_n). The layers were fabricated according to method (i). μ decreases with increasing d_n. A semi-logarithmic function is found in agreement with the theory given in Ref. [35]. The curves show, that the RPP is equivalent to platinum, and that PC leads to lower results in comparison to acetonitrile. The electrodeposition of polypyrrole onto graphite felt (contacted by RPP) leads to an improvement of μ, even without bromide catalysis, as also shown in Fig. 2.

Most depositions were performed in 0.2 M $LiClO_4$/PC, which was found to be a good compromise for both electrodes (cf. Discussion and Fig. 13). However, it should be mentioned, that PC is not an ideal solvent, as it may react with the protons generated in the course of the anodic oxidation [37]. Somewhat contradicting results are reported, namely a good stability of this solvent up to 2 V versus SHE [38] in the absence of salts and an anodic oxidation at 1 V versus SHE [39], both on platinum.

Two examples of the cyclic behaviour of the single PPy electrode are given in Fig. 3, e.g. a stable cyclic behaviour is found for a 100 μm PPy layer in both cases. In general, the current efficiency is 100%. The active mass utilization depends strongly on the nominal thickness of the PPy layer and on the solvent. The salt has nearly no influence. It is believed, that this is a matter of specific viscosity. In the viscous solvents, transport of the counter ions in the pores is severely hindered. This is also shown in Table 1, where some results obtained by means of slow cyclic voltammetry are compared with the former results of Tanguy and co-workers [26].

3.2. Natural graphite composites

Natural graphite is a highly crystalline material. It is therefore suitable for the reversible formation of graphite intercalation compounds of the acceptor-type. Composites natural

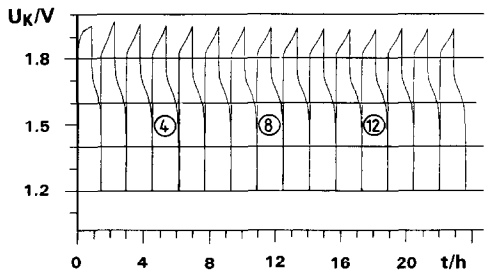

Fig. 4. Typical cyclic curves for $j = 0.5$ mA cm^{-2} for GIC single electrodes in 0.1 M NMe_4PF_6/PC. Potential limits from +1.2 V to +2.5 V. Charge limit = 1.5 C cm^{-2}.

Table 2
Current density vs. galvanostatic cycling of CPP (2 mm, large excess) in two different solvent/electrolyte systems, 0.2 M $LiClO_4$. Pre-set charge electricity = 1.5 C cm^{-2}. Evaluation at 20th cycle.

Solvent	Corrosion current density, j (mA cm^{-2})	α (%)
Acetonitrile	0.1	67
	0.2	89
	0.5	93
	1.0	95
	2.0	97
Propylene carbonate	0.1	67
	0.2	93
	0.5	95
	1.0	97
	2.0	97

Table 3
Solvent/electrolyte system (0.2 M $LiClO_4$) vs. current efficiency, α, and the active mass utilization, μ, of graphite. Potentiodyanmic cycling up to $\Delta U = 0.6$ V with respect to the intercalation potential, $\upsilon_s = 0.5$ mV s^{-1}. Thin layer electrode, natural graphite flakes pressed on RPP.

Solvent	α (%)	μ (%) on discharge
Acetonitrile	65	23
Propylene carbonate	71	30
Sulfolane	87	26

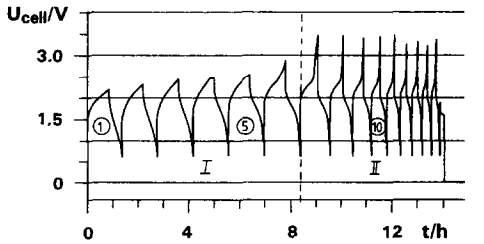

Fig. 5. Typical cyclic curves with $j = 0.5$ mA cm^{-2} for PPy/GIC single cells in 0.2 M $LiClO_4$/acetonitrile. The theoretical redox capacity of the PPy layer $Q_{00} = 4.85$ C cm^{-2}, but it was charged only to $Q_0 = 1.5$ C cm^{-2}. Cell voltage limits from +0.6 to +3.5 V.

graphite and polypropylene (CPP) were used in former investigations and in this one. Acid [13–16] and neutral [40] aqueous electrolytes were investigated in detail. More recently, aprotic solvent/electrolyte systems [41] were used. It was found that only higher stages [1] could be realized. This was attributed to the anodic oxidation of the solvent due to the very positive potential in the course of the charge process (preparation of graphite intercalation compounds (GIC) for X-ray diffraction) confirmed in the authors' laboratory. The formation of pores via salt powders (Na_2SO_4), which were leached thereafter in hot water, after removal of a surface polypropylene film, was also studied [23].

Fig. 4 displays the cyclic behaviour of a 2 mm CPP single electrode in NMe_4PF_6. This salt was selected due to its stability to avoid that there no electrolyte losses during cycling. Regular cyclic charge/discharge curves at 0.5 mA cm^{-2} are found. The conversion of the graphite is low due to its large excess in the CPP plate. The average current efficiency is only 92% between the fourth and the tenth cycles and varies strongly with the current density, as demonstrated in Table 2. It increases with increasing current densities due to the fact, that the side reaction — the anodic decomposition of the solvent molecule — goes along a relatively flat current voltage curve, while electrochemical intercalation/de-intercalation follows a steeply rising curve.

It is also due to these effects, that a strong influence of the solvent/electrolyte system on α and μ is found. Table 3 shows some examples. In this case a limited amount of graphite (graphite flakes pressed at higher temperatures as a thin layer on RPP) was provided in order to evaluate μ. The suitability of the solvents are in the following order: sulfolane > propylene carbonate > acetonitrile.

3.3. Single cells

The cyclic behaviour of single cells was studied in detail. CPP was used in a large excess with respect to PPy (factor of 100). As pointed out below, the cell capacity was limited by the negative electrode, and side reactions at the positive electrode could be evaluated with high sensitivity. Cycling of the cell began with a first charge, (Eq. (1)), as PPy is synthesized in the doped form. The charge was limited to 1.5 C cm^{-2}, corresponding to 31% of the whole PPy redox capacity. Thus, the 100 μm thick PPy layer on RPP was only partially converted at the beginning ($Q_0 = 1.5$ C cm^{-2} charge versus $Q_{00} = 4.85$ C cm^{-2} theoretical redox capacity).

Fig. 5 displays typical cyclic charge/discharge curves for a formed CPP and a 100 μm PPy layer in 0.2 M $LiClO_4$ in *acetonitrile*. The negative electrode was directly used, it was not initially discharged and 1–2 times cycled prior to the experiment. Two characteristic sections can be recognized, I and II, respectively. The cyclic behaviour is nearly constant during the short period I. But redox capacity decays rapidly in the course of section II.

As already discussed in Section 3.2., the anodic stability of acetonitrile is relatively poor. Section I is only up to the

[1] 'Stage' is a relative measure for the anion concentration in the GIC: C_{24}: first stage, C_{48}: second stage, etc.

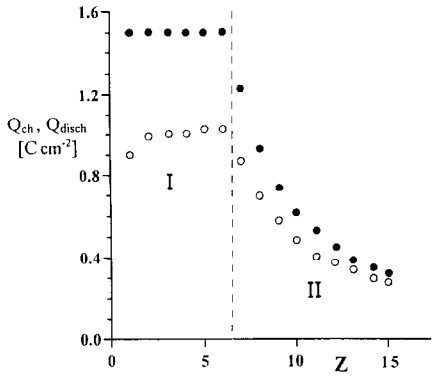

Fig. 6. Evaluation of cycling experiment shown in Fig. 7, (●) charge and (○) discharge capacity on cycle number. Discrimination between section I and II is also shown.

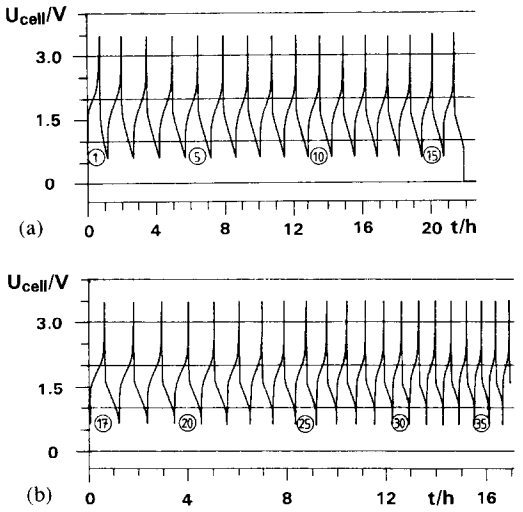

Fig. 7. Typical cyclic curves for $j = 0.5$ mA cm^{-2} for PPy/GIC single cells in 0.2 M $LiClO_4$/PC. Q_0 and Q_{00} as in Fig. 5. Cell voltage limits from +0.6 to +3.5 V.

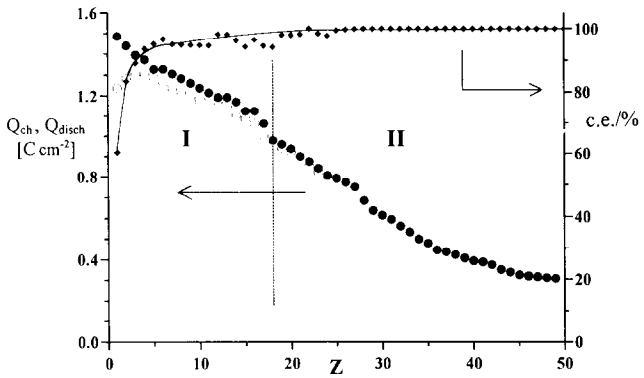

Fig. 8. Evaluation of cycling experiment shown in Fig. 5, (●) charge and (○) discharge capacity and (♦) current efficiency on cycle number. Discrimination between section I and II is shown.

sixth cycle. The current efficiency is only 70%. It is possible to apply the full charge in this case, namely 1.5 C cm^{-2}. Active mass utilization of the PPy for this solvent is high, 45% at $d_n = 100$ μm, cf. Fig. 2 [23], finally, the PPy stock is exhausted. Thereafter, the decreasing section II is beginning.

A good approach to the ideal model presented in the Discussion can be realized in this case, see Fig. 6. The separation of the sections I and II can be observed.

If *propylene carbonate* is used as solvent, and all other parameters are not changed, then another result is obtained. Up to the 17th cycle, the redox capacity decreases continuously, but at a low rate. The current efficiency was about 95% from the 5th to the 15th cycle. It was not possible, however, to apply the full charge, 1.5 C cm^{-2}, to the system, even in this section. It can be recognized, that Q_{ch} is lower, down to about 1.2 C cm^{-2}. Limitation is due to an early increase in the cell voltage to the preset upper limit, 3.5 V. The reason for that is the relatively low active mass utilization of PPy for PC electrolytes, about 20%, see Fig. 2, according to only about 1.0 C cm^{-2} that can be expected, in rough accordance to Fig. 7. Some anodic decomposition of PC may play an additional role. Beginning with the 18th cycle the redox capacities decreased further, but at a higher rate. Thus two characteristic sections, I and II, can be recognized again, as shown in Fig. 8. A similar restriction is found for porous CPP [23], again in PC. For a CPP plate, with 25% pore builder (Na_2SO_4), 85% degree of leaching, section I dropped down to seven cycles, the current efficiency was 83%. The reason for this can be understood in the light of the decrease of the cycling efficiency at the GIC electrode with decreasing true current densities, see Table 2.

Fig. 9 shows another interesting feature, acquired with the 20 cm^2 plate and frame cell. As already mentioned, the interelectrode gap was about 1 mm, in comparison with the 10 mm in the case of the glass cell. The medium discharge voltage increased to 1.5 V, while it was at the 1.1 V formerly. The current efficiency was 77%. The first ten cycles were not PPy-limited due to the application of graphite felt (GDF 2) modified negative electrodes.

Electrodeposition of PPy onto this material was possible without bromide catalysis [23]. Cycling and active mass utilization of this arrangement was highly efficient. Begin-

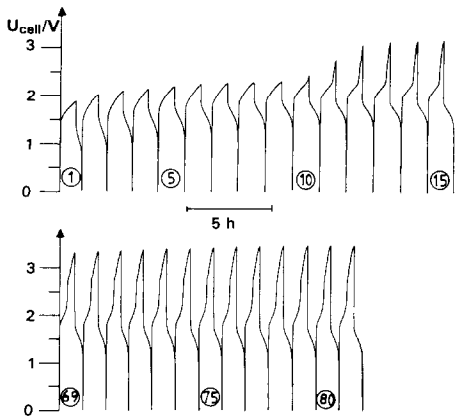

Fig. 9. Typical curves with $j = 0.5$ mA cm^{-2} for PPy/GIC single cells in 0.2 M $LiClO_4$/PC. The PPy was electrodeposited on a RPP/graphite felt electrode. A plate and frame cell with an surface area of 20 cm^2 and an electrode distance of 1 mm was used. Q_0 and Q_{00} as in Fig. 5. Cell voltage limits from 0 to +3.5 V.

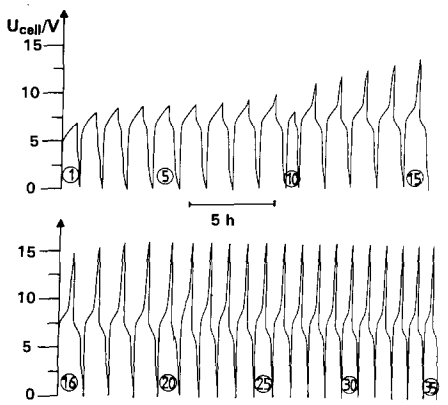

Fig. 10. Typical cyclic curves with $j = 0.5$ mA cm^{-2} for PPy/GIC bipolar battery with four bipolar electrodes and two end electrodes in 0.2 M $LiClO_4$/PC. Q_0 and Q_{00} as in Fig. 5. Cell voltage limits from +0 to +16 V.

ning with the 11th cycle, a reaction occurs at another potential in addition on charging the cell. It is probably hydrogen evolution. As hydrogen cannot be recycled, the current efficiency drops to 54%.

The last example is due to *sulfolane* as solvent. As already shown in Table 1, the active mass utilization drops down to a few percents in this viscous solvent/electrolyte system. This behaviour is totally reflected in the cyclic behaviour of cells in 0.2 M $LiClO_4$/sulfolane. The PPy-layer thickness was 37 μm in this case. Reversible cycling was possible, but only at a level of 0.056 C cm^{-2} between 0 and 2.2 V. This is about 3% of the theoretical redox capacity. The cell is strongly limited by the negative electrode.

3.4. Bipolar battery

The relative high resistivity of RPP (~40 Ω cm) leads to the application of 0.5 mm thick bipolar electrodes. The battery consisted of five bipolar cells. It was prepared and cycled under the same conditions as the 20 cm^2 single plate and frame cell, but between 0 and 16 V. The total cell voltage on discharge was as high as 7.0 V. As shown in Fig. 10, in addition to the 'structure' of the charge curve, the discharge curve began to develop some irregularities from the beginning. After 35 cycles, the redox capacity had decreased to ~50%.

4. Discussion

The results demonstrate the feasibility of an entirely metal-free rechargeable battery on the basis of PPy/GIC. It is one of the first examples of a metal-free battery with a cell voltage of above 1 V. In the following, the discussion is divided in two sections. Section 4.1 describes the interaction of single electrode processes in a secondary cell. In Section 4.2, the problems connected with the novel system and their solution are summarized.

4.1. Interaction of single electrode processes in a secondary cell

The occurrence of the two sections I and II as shown in Fig. 6 can be rationalized according to Fig. 11. Mole numbers n of active materials are plotted versus a relative time axis Q; galvanostatic charge and discharge are assumed to be applied. Individual current efficiencies λ and ϵ are introduced [42,43], while commonly only Ah efficiencies α are used, defined for the complete cell according to Eq. (2).

Charging an individual electrode is performed with the electrode current efficiency, λ:

$$n = \lambda \frac{Q_{ch}}{zF} \tag{4}$$

where n is the number of moles of the active material, z the electron number and F the Faraday constant. On the other hand, discharge is according to the electrochemical current efficiency, ϵ:

$$Q_{disch} = \epsilon n z F \tag{5}$$

The Ah efficiency α can be derived:

$$\alpha = \frac{Q_{disch}}{Q_{ch}} = \epsilon\lambda \tag{6}$$

Thus, α becomes inefficient, if one or both electrode current efficiencies are below unity, and the cycleability of the cell is only possible if [42,43]:

$$\alpha_+ = \alpha_- \tag{7}$$

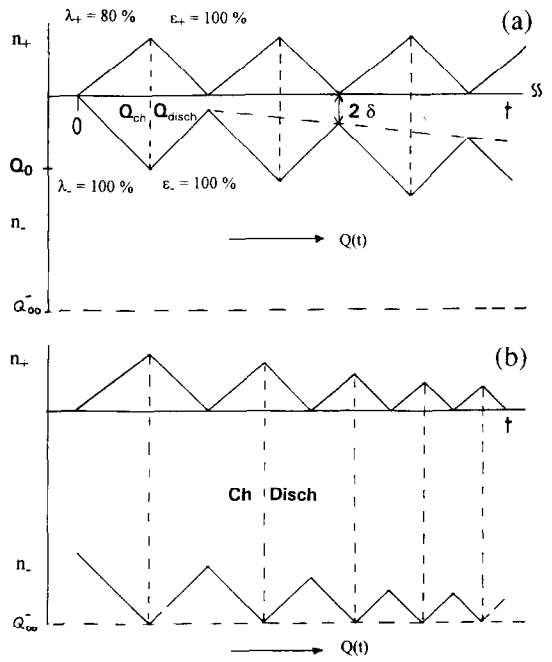

Fig. 11. Model for the cyclic behaviour of a PPy/GIC single cell. It is assumed, that $\lambda_+ = 80\%$, the other current efficiencies are quantitative and $Q_{00}^- = 3\,Q_0^-$, (a) Phase I, (b) phase II.

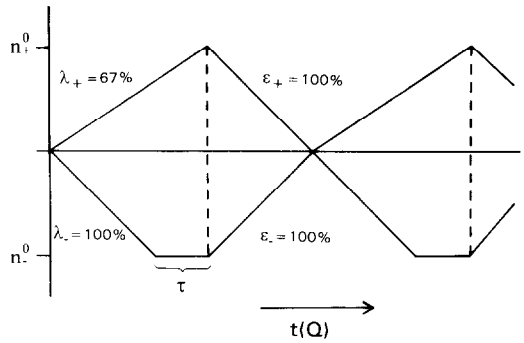

Fig. 12. Model for the cyclic behaviour of a PPy/GIC cell. It is assumed that $\lambda_+ = 67\%$ and the other current efficiencies to be quantitative. A reductive side reaction of the solvents starts as soon as the state of charge n_-^0 is reached.

Otherwise, non-reacted active materials will accumulate at one side. This behaviour can easily be modelled according to Fig. 11. It is assumed, that charging process of the positive electrode has only a λ_+ of 80%. In the section II, the continuous decrease can be formulated if Q_0 is the capacity at the end of section I. For the first cycle in section II, it will be:

$$Q_1 = \alpha Q_0 \tag{8}$$

and for the second cycle:

$$Q_2 = \alpha Q_1 = \alpha^2 Q_0 \tag{9}$$

and after Z cycles in section II the capacity has decreased to:

$$Q_z = \alpha^Z Q_0 \tag{10}$$

If Q_{00}^- is the pre-set theoretical capacity at the negative electrode, the number of possible cycles within section I can be easily derived from Fig. 11:

$$Z_1 = \frac{Q_{00}^- - Q_0}{\delta} \tag{11}$$

where δ is the deficit arising along all cycles in section I due to the non-quantitative λ_+.

It is possible to re-oxidize the PPy negative electrode periodically against an auxiliary electrode to the entirely doped state. Thus, period II can be eliminated. However, such measures are generally unpracticable, as in similar cases in battery engineering. More promising from a practical point of view is another strategy, see Fig. 12. A cathodic decomposition of water (as a component of the electrolyte) is assumed along part τ. A perfect cyclic behaviour is obtained. The decomposition product (hydrogen) does not accumulate in the cell.

4.2. Parameters and problems in the cell

4.2.1. Optimum solvent/electrode system

PC was found to be a compromise on the search of an optimum solvent/electrolyte system. As shown in Fig. 13, sulfolane is optimum for GIC, but it is very poor for PPy. Acetonitrile is optimum for PPy but it is heavily oxidized on GIC. It is mentioned in the literature that aprotic solvents are oxidized on oxide electrodes [8,19]. This can be explained by the catalytic action of such oxide electrodes for the anodic oxidation. But graphite has no electrocatalytic properties and it is surprising that it exerts also an anodic side reaction. The anodic oxidation of these molecules was studied recently in detail by measurements on a rotating disc ring electrode [34]. Protons are injected on the disc where an anodic oxidation, according to Eq. (12), takes place and they are identified at the cathodically polarized ring:

$$CH_3OH + H_2O \longrightarrow CO_2 + 6H^+ + 6e^- \tag{12}$$

The methanol oxidation is shown as a simple example, the real nature of the anodic decomposition of the solvents used is not known. But the same rate of proton injection, 1 mole H^+ for one Faraday, is maintained. The method was first described in Ref. [44]. In accordance to our battery findings, the ranking in terms of minimization of this side reaction was found at GIC: PC, sulfolane > acetonitrile > butyrolactone, 2-methyltetrahydrofuran, ethlyene carbonate/PC > NMP. The kind of the supporting electrolyte, cations like Li^+, NEt_4^+, NBu_4^+ and anions like ClO_4^-, BF_4^-, PF_6^-, seems not to be critical. None of these ions are either reduced or oxidized in the range of the battery operation.

4.2.2. Current density

Current density plays a strong role. As already mentioned in Section 3.3, this is due to the relative flat form of the current–voltage curve for solvent decomposition in comparison to the steeply rising curve for GIC. A problem arises due to the widely varying active mass utilization of the PPy electrode. μ can be the limiting factor in extreme cases, as shown in some examples. Various strategies to improve the porosity and thus the active mass utilization μ were established [23].

4.2.3. Residual bromide

The presence of residual bromide in the porous PPy electrode may lead to a partial electrochemical short-circuit and should be omitted. As this is not easy feasible, the uncatalyzed deposition on graphite felt is preferred in our recent work.

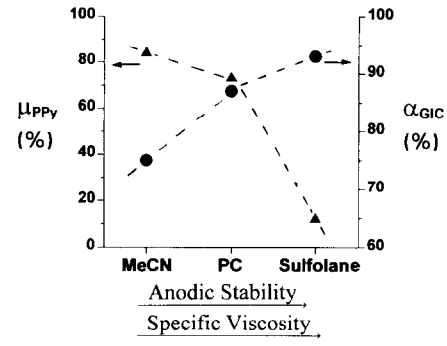

Fig. 13. A comparison of three solvents with respect of the active mass utilization, μ, for the PPy layer ($d_n = 10$ μm) and the current efficiency, α, on cycling of GIC at a current density of 0.5 mA cm^{-2}. Electrolyte: 0.2 M $LiClO_4$. MeCN = acetonitrile.

Table 4
Corrosion current densities, j_{corr}, of GIC in aprotic solvent/electrolyte systems

Solvent	Electrolyte (0.2 M)	j_{corr} (μA cm^{-2})
Acetonitrile	$LiClO_4$	20
Acetonitrile	NEt_4ClO_4	14
Acetonitrile	NEt_4BF_4	[a]
Propylene carbonate	$LiClO_4$	16
Propylene carbonate	NEt_4ClO_4	16
Propylene carbonate	NEt_4BF_4	20
Sulfolane	$LiClO_4$	1.5
Sulfolane	NEt_4ClO_4	3
Sulfolane	NEt_4BF_4	8

[a] Poisoning of the electrode by the decomposition products.

4.2.4. Residual monomers

Another problem may arise due to residual monomers in the porous polypyrrole. It may diffuse to GIC, where it forms PPy. A solution of this drawback was found in a second step potentiostatic after polymerization at the PPy electrode in a monomer-free electrolyte.

4.2.5. Overcharge/overdischarge features

A brief analysis of the overcharge/overdischarge features must be added. PPy can be reversibly cycled in the potential range from 0.4 to -1.5 V versus SCE. Irreversible overoxidation proceeds at potentials positive to it, and water electrolysis (and eventually some hydrogenation of the conjugated system) may occur beyond -1.5 V. With respect to graphite, graphite oxide may be formed at the end of the anodic intercalation.

4.2.6. Self-discharge behaviour

In close connection to it is the self-discharge behaviour of the positive electrode. Corrosion behaviour of the GIC electrode was already studied in detail in Ref. [45]. It was measured by galvanostatic cycling of single electrodes through variation of the rest time τ at open-circuit potential prior to discharge. A plot of α versus τ leads to straight, declining lines. Therefrom, the corrosion current density, j_{corr}, can be easily evaluated:

$$j_{corr} = \frac{\Delta\alpha}{\Delta\tau} Q_{charge} \qquad (13)$$

The results are compiled in Table 4. In accordance to the cyclic behaviour of the GIC single electrodes and the cells, (see Sections 3.2 and 3.3), sulfolane yields the lowest corrosion rates of GIC, while the other two solvents have an almost similar action. The mechanism probably consists of a superposition of an anodic oxidation of the solvent and a cathodic deintercalation of the electrode.

5. Conclusions

The secondary battery with doped polypyrrole layer and composite natural graphite/polypropylene suffers from a somewhat low electrochemical equivalent of the active materials, see Table 5. The theoretical energy density is about 80 Wh kg^{-1} according to Eq. (1), $\nu = \nu' = 0$. It is expected, that a relatively high portion of this value can be really utilized by extensive application of thermoplastic and graphite/carbon technologies to yield practical energy densities of 20–30 Wh kg^{-1}.

Table 5
Comparison of data for the lead/acid accumulator and the PPy/GIC accumulator

Parameters	$Pb/PbO_2/H_2SO_4$	$PPy/C_{24}/PC + LiClO_4$
m_e (−) (Ah kg^{-1}) [a]	259	91
m_e (+) (Ah kg^{-1}) [a]	224	93
U_H^+ (V) (SHE)	1.68	1.9
U_H^- (V) (SHE)	−0.35	0.2
U_0/V (cell	2.03	1.7
$E_{s,th}$ (Wh kg^{-1})	170	80
$E_{s,pract}$ (Wh kg^{-1})	30–40	20–30

[a] Electrochemical equivalents of the negative and positive active materials.

The battery contains two intercalation electrodes of the acceptor-type. This is in analogy to the two donor-type intercalation electrodes, which usually make up the rechargeable lithium batteries. An inherent drawback of such systems is their relatively 'soft' charge/discharge characteristics. It resembles to a capacitor rather than to an electrochemical power source, but it has a finite open-circuit voltage after discharge.

The main problem in connection to the metal-free electrodes can be clearly identified after this research project. The positive (GIC) electrode has an extreme potential, and this leads to some anodic attack of the aprotic solvents. An alternative would be the polythiophene electrode with a potential more negative by ~0.5 V. This is presently investigated by the same methods. Unfortunately, the costs will be higher. But the ultimate cell voltage remains above 1 V. There is also an option to improve the negative electrode. It was found, that PPy is well cycleable in 10 M H_2SO_4 in CH_3COOH. As graphite forms an intercalation compound of stage I in this electrolyte, albeit at somewhat more negative potentials [8], and can be cycled therein, these finding opens a way to build a rechargeable battery in a protic, well-conducting and nonexpensive electrolyte. Unfortunately, the active mass utilization of the porous electrodes is low due to the relatively high viscosity of this electrolyte.

The authors developed, in parallel, a second metal-free rechargeable cell with aqueous electrolytes, e.g. 50% H_2F_2. The cell voltage is about 1.7 V [20,21,46].

Acknowledgements

Financial support by AIF (Ministry of Economics, Bon) and by MWF (Ministry of Science and Research, Düsseldorf) is gratefully acknowledged.

References

[1] E.J. Wade, *Secondary Batteries: Their Theory, Construction and Use*, The Electrician Printing and Publishing Company, London, 1902.
[2] B. Scrosati, *J. Electrochem. Soc., 139* (1992) 2776.
[3] D. Fauteux and R. Kocksbang, *J. Appl. Electrochem., 23* (1993) 1.
[4] H. Alt, H. Binder, A. Köhling and G. Sandstede, *J. Electrochem. Soc., 12* (1971) 1950.
[5] H. Alt, H. Binder, A. Köhling and G. Sandstede, *Electrochim. Acta, 17* (1972) 873.
[6] H. Alt, H. Binder, A. Köhling and G. Sandstede, *DE Patent No. 2 240 614* (8/1972) (Battelle, Frankfurt/Main).
[7] G. Matricicali, M.M. Dieng, J.F. Dufeu and M. Guillou, *Electrochim. Acta, 21* (1976) 943.
[8] F. Beck, T. Boinowitz and U. Tormin, *DECHEMA-Monogr., 128* (1993) 287.
[9] F. Beck, *8th Int. Symp. 'Notstromversorgung', 11–12 Mar. 1993, Munich, Germany*, p. 357ff.
[10] F. Beck, in H. Gerischer and C.W. Tobias (eds.), *Advances in Electrochemical Science and Engineering*, Vol. 5, VCH, Weinheim, 1995.
[11] R. Bittihn, G. Ely, F. Woeffler, H. Münstedt, H. Naarmann and D. Naegele, *Makromol. Chem., Macromol. Symp., 8* (1987) 51.
[12] H. Münstedt and H. Gebhardt, *DE Patent No. 3 545 902* (12/1985) (BASF).
[13] F. Beck and H. Krohn, *J. Power Sources, 12* (1984) 9.
[14] F. Beck and H. Krohn, *Synth. Met., 14* (1986) 137.
[15] R. Fujii, *Rep. Government Industries Research Institute, Osaka, Japan, 353* (1978) 1.
[16] W. Rüdorff and U. Hofmann, *Z. Anorg. Allg. Chem., 238* (1938) 1.
[17] V. Haddadi-Asl, M. Kazacos and M. Skyllas-Kazacos, *J. Appl. Electrochem., 25* (1995) 29.
[18] F. Beck and G. tom Suden, *Electrochim. Acta*, (1995) in press.
[19] D. Guyomard and J.M. Tarascon, *J. Electrochem. Soc., 139* (1992) 937.
[20] F. Beck, T. Boinowitz, H. Krohn, U. Tormin and E. Ther, *Mol. Cryst. Liq. Cryst., 245* (1994) 177.
[21] F. Beck, T. Boinowitz, H. Krohn, E. Ther and B. Wermeckes, *The Electrochemical Society Fall Meet., Miami Beach, FL, USA, 9–14 Oct. 1994*, Abstr. No. 152.
[22] F. Beck, H. Krohn and W. Kaiser, *J. Appl. Electrochem., 12* (1982) 505.
[23] F. Beck, T. Boinowitz, G. tom Suden and E. Abdelmula, *GDCh-Monogr., 2* (1995) 223.
[24] F. Beck and A. Pruß, *Electrochim. Acta, 28* (1983) 1847.
[25] F. Beck, H. Krohn, S. Rashwan and I. Litzenberger, *J. Power Sources, 32* (1990) 287.
[26] M. Slama and J. Tanguy, *Synth. Met., 28* (1989) C139; N. Mermilliod, J. Tanguy and F. Petiot, *J. Electrochem. Soc., 133* (1986) 1073.
[27] M. Oberst and F. Beck, *Angew. Chem., 99* (1987) 1061.
[28] F. Beck and M. Oberst, *J. Appl. Electrochem., 22* (1992) 332.
[29] R. Bittihn, *Kunststoffe, 79* (1989) 530.
[30] N. Nagashima, T. Mine, Y. Ikezawa and T. Takamura, *J. Power Sources, 43/44* (1992) 611.
[31] W.A. Wampler, Ch. Wei and K. Rajeshwar, *J. Electrochem. Soc., 141* (1994) L13.
[32] T. Grcev, M. Cvetkovska and T. Obradovic, *Ext. Abstr., 44th Meet. International Society of Electrochemistry (ISE), Berlin, Germany, Sept. 1993*, Abstr. No. 1.7.11.
[33] B.M. Coffey, P.V. Madsen, T.O. Poehler and P.C. Searson, *184th Meet. The Electrochemical Society, New Orleans, LA, USA, Oct. 1993*, Abstr. No. 375.
[34] T. Boinowitz, *Ph.D. Thesis, University Duisburg, Germany, 1995.*
[35] R. Penner and C. Martin, *J. Electrochem. Soc., 133* (1986) 2206.
[36] K. Mund and F. von Sturm, *Electrochim. Acta, 20* (1975) 463.
[37] J. Hlavaty and P. Novák, *Electrochim. Acta, 37* (1992) 2595.
[38] S. A. Campbell, C. Bowes and R.S. McMillan, *J. Electroanal. Chem., 284* (1990) 195.
[39] B. Rasch, E. Cattaneo, P. Novak and W. Vielstich, *Electrochim. Acta, 36* (1991) 1397.
[40] H. Krohn, F. Beck and H. Junge, *Ber. Bunsenges. Phys. Chem., 86* (1982) 704.
[41] Z. Zhang and M.M. Lerner, *J. Electrochem. Soc., 140* (1993) 742.
[42] F. Beck, in A.T. Kuhn (ed.), *The Electrochemistry of Lead*, Academic Press, London, 1979.
[43] F. Beck and K.-J. Euler, *Elektrochemische Energiespeicher*, VDE-Verlag, Berlin, 1984.
[44] F. Beck and M. Oberst, *J. Electroanal. Chem., 285* (1990) 177.
[45] F. Beck, H. Krohn and E. Zimmer, *Electrochim. Acta, 31* (1986) 371.
[46] H. Krohn, E. Ther, U. Tormin, B. Wermeckes and F. Beck, *Proc. NATO Advanced Research Workshop on New Promising Electrochemical Systems for Rechargeable Batteries, Kiev, Ukraine, 14–18 May 1995*, Kluwer, Dordrecht, 1995, in press.